Group-theoretic spectrum analysis of hexagonal city distributions in Southern Germany and Eastern USA

Kiyohiro Ikeda and Kazuo Murota and Yuki Takayama and Motohiro Kamei

Department of Civil and Environmental Engineering, Tohoku University, School of Business Administration, Tokyo Metropolitan University, Kanazawa University, East Nippon Expressway Company Limited

19 September 2016

Group-theoretic spectrum analysis of hexagonal city distributions in Southern Germany and Eastern USA

Kiyohiro Ikeda,[1] Kazuo Murota,[2] Yuki Takayama,[3] Motohiro Kamei[4]
[1]*Department of Civil and Environmental Engineering, Tohoku University, Aoba, Sendai 980-8579, Japan*
[2]*School of Business Administration, Tokyo Metropolitan University, Hachiohji, Tokyo 192-0397, Japan*
[3]*Kanazawa University, Kakuma, Kanazawa 920-1192, Japan*
[4]*East Nippon Expressway Company Limited, Mihama, Chiba 261-0014 Japan*
(Dated: September 19, 2016)

Hexagonal distributions of cities of various sizes in Southern Germany are envisaged in central place theory. Yet scientific verification of this theory has been lacking. To scientifically support this theory, we propose a group-theoretic double Fourier spectrum analysis procedure that can detect geometrical patterns in population distributions of cities. In addition to hexagonal patterns in the theory, we propose megalopolis patterns. Using this procedure, strong power spectra for megalopolis patterns were detected for population data in Southern Germany. Moreover, a gigantic hexagonal distribution of cities in Eastern USA was found to be an assemblage of megalopolis and hexagonal patterns. The amazing geometrical regularity of this distribution manifests the existence of these patterns in the real world, thereby underpinning central place theory.

PACS numbers: 02.30.Oz, 05.65.+b, 89.65.Lm, 89.75.Kd

Cities are cradles of economic development and are prospering worldwide with a tendency for more and more people to live there [1], leading to a problematic increase in human population density [2]. Extensive studies of cities have been conducted from various points of view: size (based mainly on Zipf's law) [3–7], scaling [8–10], geometry (fractal) [11, 12], geometry (growth pattern) [13–16], sociodynamics [17], spatial economy [18–20], and geographical distribution [8, 21] of cities. This letter focuses on the geographical distribution of cities as elucidation of its mechanism would be vital for the successful design of the location of future urban infrastructures.

In central place theory in economic geography, self-organization of a hexagonal distribution in a hierarchy of urbanization (megalopolises, cities, towns, villages, etc.) was envisaged based on a study of Southern Germany by Christaller in 1933 [8] (Fig. 1(a)) and a distribution comprising overlapping hexagons of different sizes was proposed by Lösch [21] (Fig. 1(b)). The importance of that theory in the understanding of distributions of cities is well acknowledged and several attempts to simulate the self-organization of central place systems have been conducted through modeling of economic agglomerations [19, 22]. Yet scientific verification of the existence of hexagonal agglomerations in the real world has been lacking, notwithstanding extensive attempts at such verification [3–20].

This letter aims to verify the existence of hexagonal agglomerations in the real world by a novel and rare study unifying natural and social sciences. To this end, we refer to studies of self-organization of hexagonal population distributions on a hexagonal lattice [23, 24] and to those of various physical phenomena [25–27], as well as central place theory [8, 21]. From a physical standpoint, hexagonal patterns of cities located in large flat areas should be self-organized through pattern formation. Moreover,

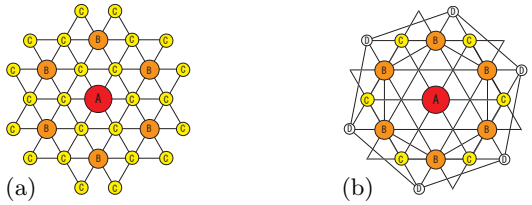

FIG. 1. (a) A distribution of Christaller. (b) Three overlapping smallest hexagons of Lösch. A larger circle expresses a larger place.

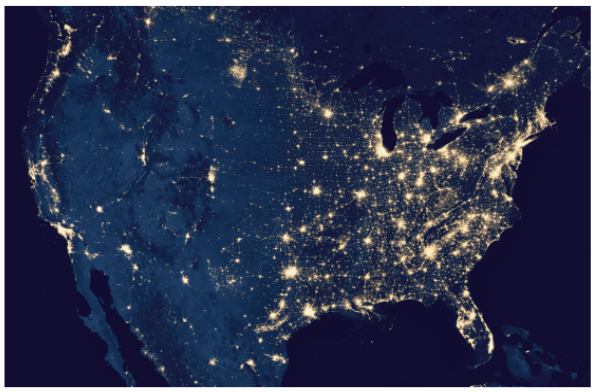

FIG. 2. City lights of USA taken by Suomi NPP satellite [28].

for verification, we propose a group-theoretic spectrum analysis to detect spatial patterns in real population data based on those studies. As targets of this analysis, we focus on Southern Germany and Eastern USA. This letter poses a question: "Does a hexagonal distribution exist in Southern Germany as envisaged by Christaller?" Using the present analysis procedure, such a distribution was in fact detected in Southern Germany, the origin of central place theory [8]. Moreover, this letter attempts to find overlapping hexagonal distributions of cities as envisaged by Lösch [21] in a large area in Eastern USA.

The city lights of the USA display apparent geometrical patterns that have motivated this study of the formation of these patterns (Fig. 2 [28]).

Spectrum analysis is a standard scientific tool to detect the occurrence of pattern formation. This letter proposes a group-theoretic spectrum analysis procedure to detect hexagonal distributions in real population data. Instead of a naïve double Fourier series in rectangular coordinates, we employ an oblique Fourier series on a finite hexagonal lattice with periodic boundary conditions [29] and regroup the series into so-called *isotypic components*, which are related to hexagonal patterns of various kinds [24, 27]. The population distribution $\boldsymbol{\lambda}$ on the lattice is expanded into a special form [30]:

$$\boldsymbol{\lambda} = \sum_{m \in \mathrm{L_{hexa}}} \boldsymbol{q}^{(m)}$$

in which each m labels a different isotypic component, $\mathrm{L_{hexa}}$ is a set of m, and $\boldsymbol{q}^{(m)} \equiv \sum_{i=1}^{M(m)} c_i^{(m)} \boldsymbol{q}_i^{(m)}$. Here, $M(m)$ is the number of the basis vectors for m, $c_i^{(m)}$ is a Fourier coefficient, and $\boldsymbol{q}_i^{(m)}$ is a Fourier term.

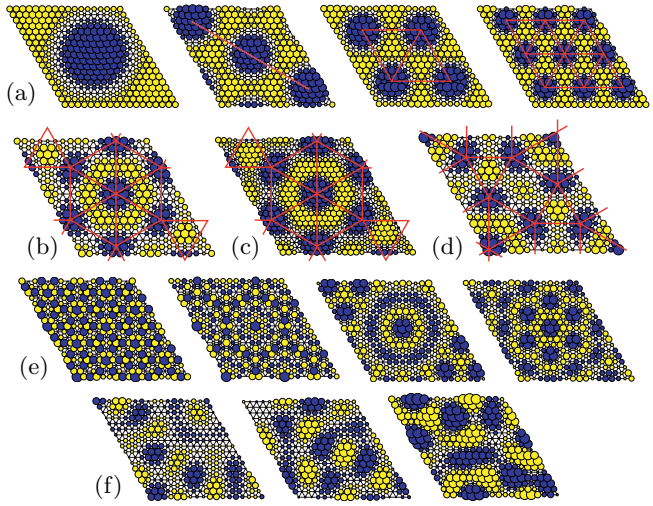

FIG. 3. Patterns on an 18×18 hexagonal lattice expressed by $\boldsymbol{q}^{(m)}$. (a) Hexagons. (b) Megalopolis. (c) Megalopolis on a 24×24 mesh. (d) Shifted megalopolis. (e) Other bifurcating patterns. (f) Non-bifurcating patterns. A blue circle denotes a positive component, a yellow circle indicates a negative one, the area of a circle expresses the magnitude of the component, and a red line is used to clarify spatial patterns.

While patterns expressed by $\boldsymbol{q}^{(m)}$ for general values of the Fourier coefficients $c_i^{(m)}$ are not necessarily bifurcating patterns self-organized from a uniform state, the following bifurcating patterns [24] play an vital role in the search of city distributions. The hexagonal patterns, which are called $\boldsymbol{q}^{\mathrm{Mono-center}}$, $\boldsymbol{q}^{3\ \mathrm{hexagons}}$, $\boldsymbol{q}^{4\ \mathrm{hexagons}}$, and $\boldsymbol{q}^{9\ \mathrm{hexagons}}$ herein (Fig. 3(a)), are interpreted as being a one-level hierarchy in central place theory because identical blue circular zones expressing agglomeration are repeated regularly. The "megalopolis pattern," termed $\boldsymbol{q}^{\mathrm{Megalopolis}}$, represents a large circle at the center, surrounded by six smaller ellipses (Fig. 3(b). The pattern

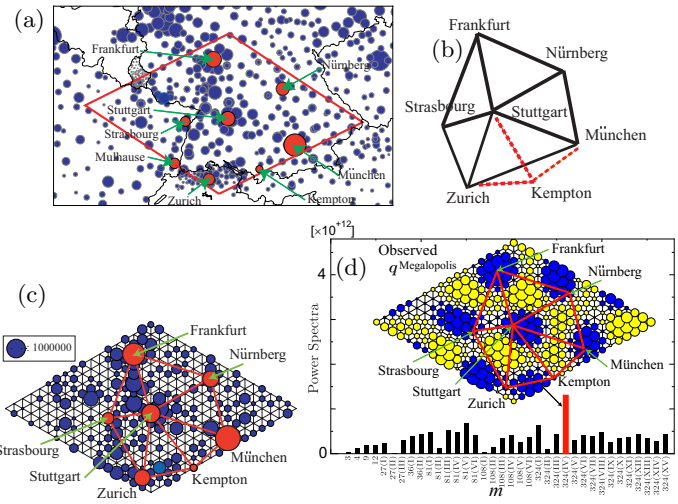

FIG. 4. (a) The domain used for the spectrum analysis of the population of Southern Germany and neighboring countries. The area of a circle denotes the population size. The population data of cities (Table A2) were taken from the City Population website (http://www.citypopulation.de/), which is based on original sources (Table A3). The latitude and longitude of a location were acquired by GoogleMap and Nominatim of OpenStreetMap (https://nominatim.openstreetmap.org/). (b) Christaller's pentagonal distribution of cities [8] shown by solid lines and added distribution by the present study shown by the dashed lines. (c) Population map and a distribution of cities plotted on an 18×18 hexagonal lattice. A series of red lines denotes the distribution of cities. (d) Power spectra of the squared magnitudes $||\boldsymbol{q}^{(m)}||^2$ of the assembled Fourier terms and the spatial pattern of the largest spectrum $\boldsymbol{q}^{\mathrm{Megalopolis}}$. The area of a blue circle in this pattern denotes the increase of population and that of a yellow one denotes its decrease.

is robust against the change in mesh size (Fig. 3(c). The pattern is interpreted as a two-level hierarchy with a circular downtown area (A-center) surrounded by six elliptic satellite places (B-centers). Although the pattern is beyond the scope of central place theory and is not given much attention in physics, it plays a vital role in the description of the distribution of cities. There are spatially shifted variants of these patterns (Fig. 3(d)) and other bifurcating patterns, some of which display megalopolis-like geometry (Figs. 3(e) and A4). Spatial regularity is absent in non-bifurcating ones (Fig. 3(f)).

Let us verify the existence of hexagonal agglomerations in the 2011 population data of a rhombic domain in Southern Germany (Fig. 4(a)). The distribution of cities proposed by Christaller (Fig. 4(b)) is the target of the present analysis. Spectrum analysis of the discretized data on an 18×18 hexagonal lattice (Fig. 4(c)) was conducted (Fig. 4(d)). The megalopolis pattern $\boldsymbol{q}^{\mathrm{Megalopolis}}$ has the largest spectrum among 37 $\boldsymbol{q}^{(m)}$'s, and is close to the theoretical bifurcating pattern (Fig. 3(b)). By comparison of this pattern with the real population distribu-

tion (Fig. 4(a)), it can be interpreted as being a hexagonal distribution of six cities (Frankfurt, München, and so on) surrounding Stuttgart (Fig. 4(c)). This pattern contains Christaller's pentagonal distribution (Fig. 4(b)), thereby scientifically underpinning central place theory. In this report, one more city, Kempton, is included in the distribution to arrive at the hexagonal pattern. Kempton, however, is a small city and it is no wonder that this city was overlooled by Christaller. That hexagonal pattern is skewed due to the geographical borders of the Alps towards the south and Rhine River towards the west. Although Southern Germany is the origin of central place theory, it is not flat as assumed by Christaller, and a clearer hexagonal pattern should be sought for in a wider flat area in Eastern USA.

Like the challenge of a large jigsaw puzzle with many pieces, we deal with a large number of cites in the large area of the Eastern USA. Megalopolis and hexagonal patterns found in 18 domains belonging to five regions (Fig. A5) were assembled to obtain a gigantic hexagonal distribution in the Eastern USA (Fig. 5), as explained below. This distribution encompasses many major cities there, which are classified as A- to F-centers, except for those in the Florida peninsula and the Appalachian Mountains. There is a hierarchy of sub-patterns with different geographical scales that look like the overlapping hexagons proposed by Lösch [21]. The patterns are blurred by the Appalachian Mountains, just as the hexagonal cell of Bénard convection becomes less clear near the boundary [31]. On the other hand, the Mississippi River does not influence the patterns so much.

A large hexagonal pattern exists in the West North Central Region centered on St. Louis (Figs. 6(a) and (d)). This pattern is associated with the predominant spectrum of $\boldsymbol{q}^{9\text{ hexagons}}$ (Fig. 6(b)), which is close to the theoretical one (the right of Fig. 3(a)). The pattern expresses a 3×3 hexagonal array of cities with incredible geometrical regularity, and covers a large area in the Eastern USA, encompassing Chicago (B-center), Detroit (C-center), Cincinnati, St. Louis, Kansas city (D-centers), and so on.

The clearest hexagonal distribution exists in a wide flat area in the Gulf Coast Region with four domains (Figs. 6(c) and A7), in which the megalopolis patterns $\boldsymbol{q}^{\text{Magalopolis}}$ are predominant. These patterns are compatible with each other and, in turn, can be assembled into a large hexagonal distribution with an amazing geometrical regularity from Dallas to Atlanta along the Gulf of Mexico (Fig. 6(d)). In particular, there is a clear hexagonal pattern centered on Birmingham (yellow lines in Fig. 6(d)). Thus, this wide flat area accommodates a hexagonal pattern, just as hexagonal patterns emerge from uniformity in physics. The large hexagonal distribution is found to merge compatibly with the south border of the 3×3 hexagonal distribution centered on St. Louis. The size of the former distribution is approximately half

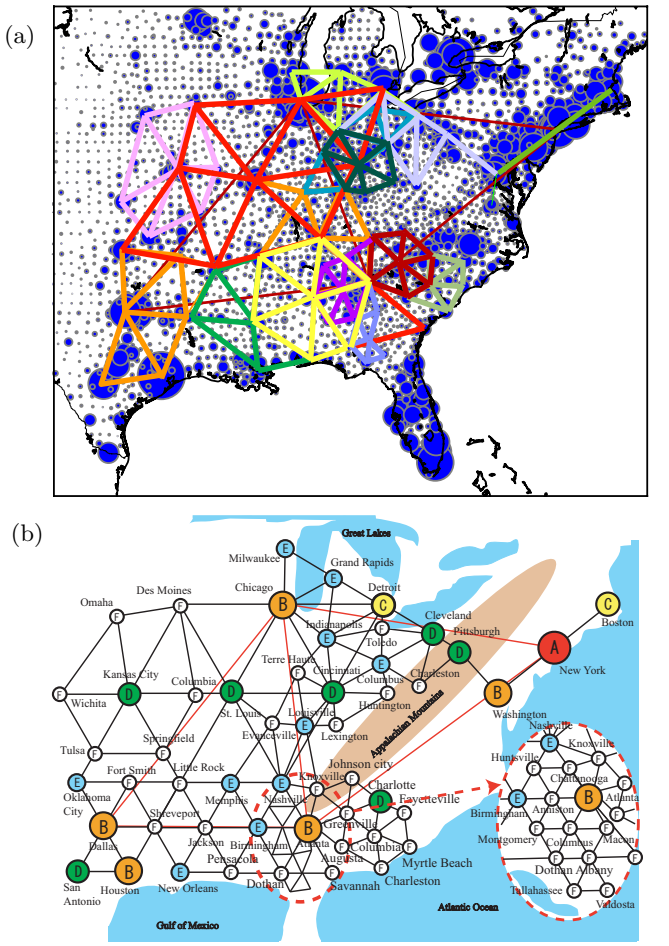

FIG. 5. (a) Assembled distribution of cities in Eastern USA drawn on a population map of that region. The area of a circle denotes the population size and lines with different colors indicate city sub-distributions. The population data of the Eastern USA in 2014 were taken from the City Population website (http://www.citypopulation.de/) (Table A4). (b) Interpretation of the distribution of cities in Eastern USA. Cities are classified from an A-center ($\lambda \geq 10,000,000$), B-centers ($5,000,000 \leq \lambda < 10,000,000$), C-centers ($3,500,000 \leq \lambda < 5,000,000$), D-centers ($2,000,000 \leq \lambda < 3,500,000$), E-centers ($1,000,000 \leq \lambda < 2,000,000$), and F-centers ($100,000 \leq \lambda < 1,000,000$) (Tables A5 and A6).

that of the latter, and has geometrical compatibility.

In the South Atlantic Region three series of fine hexagonal patterns are connected at a transportation hub at Atlanta (Figs. 5(b), 7(a), and A8). The east-bound pattern is directed towards the corridor between the Atlantic Ocean and the Appalachian Mountains, the west-bound one is connected to the hexagonal distribution in the Gulf Coast Region, and the north-bound one is connected to that in the northern industrial district. The size of these patterns is just two-thirds that in the Gulf Coast Region (Fig. 6(d)). In the industrial zone in the East North Central Region bordering the Appalachian Mountains and the Great Lakes, a T-shaped city distribution with a belt-like triangular mesh is observed (Figs. 5(b), 7(a),

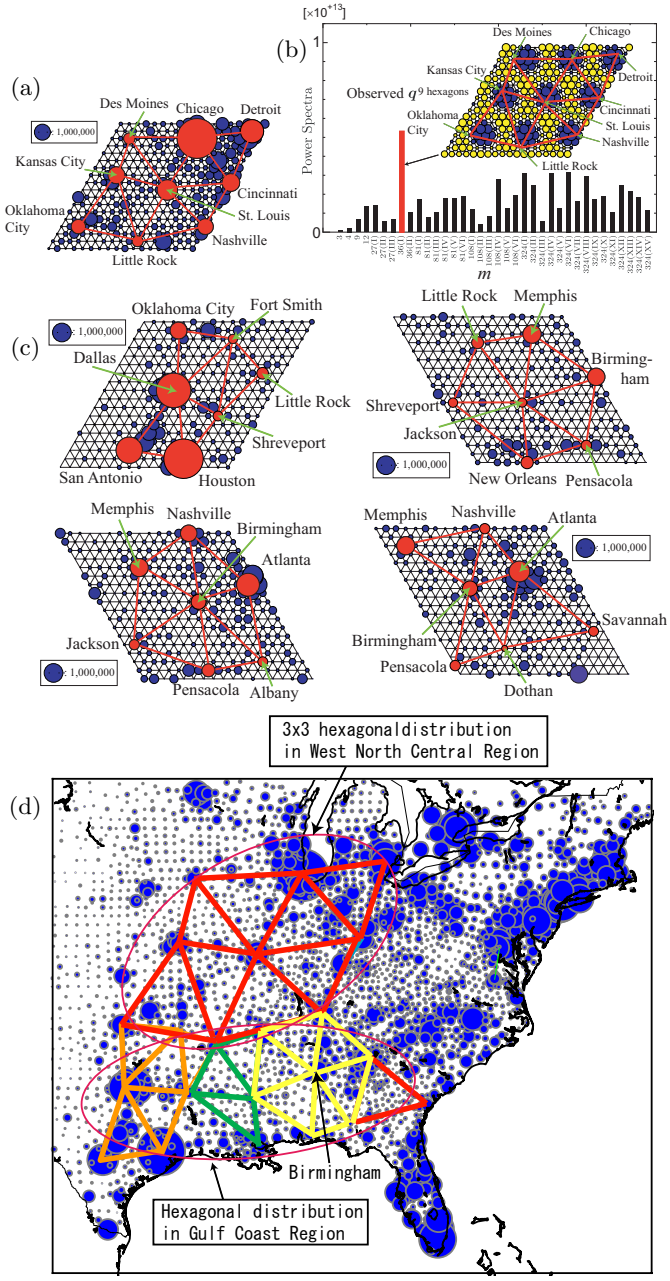

FIG. 6. Clearest hexagonal distributions of cities for West North Central and Gulf Coast Regions. (a) Distribution of cities for the West North Central Region centered on St. Louis drawn on a population map. The area of a circle denotes the population size and a series of red lines denotes the distribution of cities. (b) Power spectra of the squared magnitudes $||\boldsymbol{q}^{(m)}||^2$ of the assembled Fourier terms and the spatial pattern of the predominant spectrum $\boldsymbol{q}^{9\text{hexagons}}$ for this region. The area of a blue circle of this pattern denotes an increase of population and that of a yellow one denotes a decrease; a series of red lines denotes the distribution of cities. (c) Distribution of cities for the four domains in Gulf Coast Region drawn on population maps. (d) Assembled distributions of cities for West North Central and Gulf Coast Regions.

and A9).

The largest pattern of four rhombic cities is located in the domain of the whole Eastern USA (Fig. 7(b)): A two-level hierarchy comprising an A-center at New York City and three B-centers at Chicago, Dallas, and Atlanta is advanced in view of two competing strong spectra for $\boldsymbol{q}^{4\text{ hexagons}}$ for these four cities and $\boldsymbol{q}^{\text{Mono-center}}$ for a mono-center at New York City (Fig. A6). A line-like distribution is observed in the most agglomerated area, i.e., the Middle Atlantic Region in a closed narrow corridor between the Atlantic Ocean and the Appalachian Mountains (Figs. 7(c) and A10).

An overlapping hexagonal distribution has thus been found in Eastern USA (Fig. 5). This distribution with amazing geometrical regularity is that which was proposed by Lösch [21] (Fig. 1(b)). Among many possible spectra, only a few of them expressing megalopolis and hexagonal patterns are predominant. The authors would like to recall the book entitled "Fearful Symmetry: Is God a Geometer?," which describes the geometrical regularity of pattern formation in various physical phenomena [32]. This letter serves as a sociological experiment of pattern formation and paves the way for the application of methodologies of bifurcation theory [25–27] to the study of the geography of cities. A future task is to study the self-organization of economic agglomeration in spatial economy [18, 19] by bifurcation analysis. Since cities are complex systems with various aspects, it is vital to overcome complexity to carry out cross-fertilization of the present procedure with other scientific studies of cities [3–17].

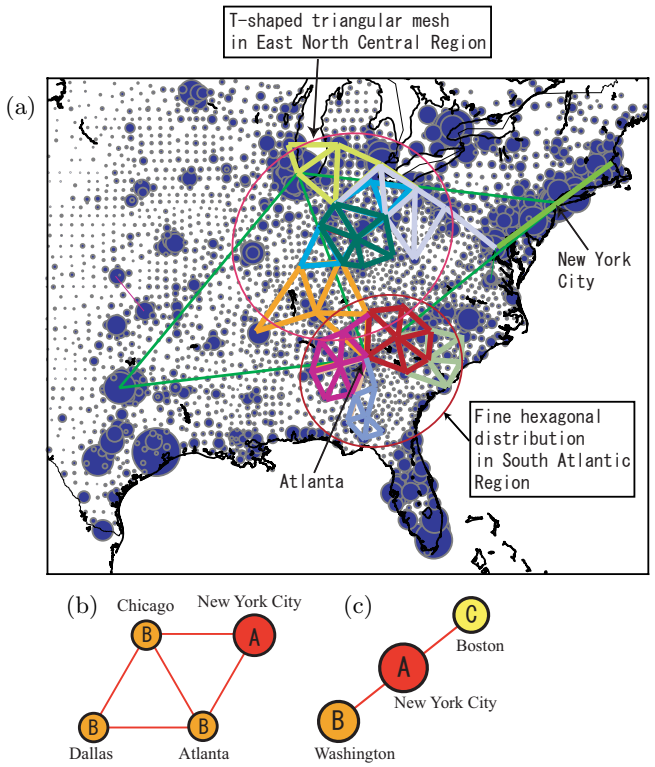

FIG. 7. (a) Distributions of cities in other regions. (b) Two-level hierarchy consisting of four large cities: New York City, Chicago, Dallas, and Atlanta. (c) A line-like distribution for the Middle Atlantic Region.

[1] N. S. Wigginton, J. Fahrenkamp-Uppenbrink, B. Wible, and D. Malakoff, Science **352**, 904 (2016).

[2] J. E. Cohen, *How many people can the Earth support?* (Norton, New York, 1995); Science **302**, 1172 (2003).

[3] G. K. Zipf, *Human Behavior and the Principle of Least Effort* (Addison Wesley, Cambridge, MA, 1949).

[4] M. Marsili and Yi–C. Zhang, Phys. Rev. Lett. **80**, 2741 (1998).

[5] X. Gabaix, The Quarterly Journal of Economics **114**, 739 (1999).

[6] T. Mori and T. E. Smith, J. Reg. Sci. **51**, 694 (2011).

[7] A. Ghosh, A. Chatterjee, A. S. Chakrabarti, and B. K. Chakrabarti, Phys. Rev. E **90**, 042815 (2014).

[8] W. Christaller, *Die zentralen Orte in Süddeutschland* (Gustav Fischer, Jena,1933). English translation: *Central Places in Southern Germany* (Prentice Hall, Englewood Cliffs, 1966).

[9] L. M. A. Bettencourt, Science **340**, 1438 (2013).

[10] M. Batty, Science **319**, 769 (2008); **340**, 1418 (2013); *The New Science of Cities* (MIT Press, Cambridge, 2013).

[11] M. Batty and P. Longley, *Fractal Cities* (Academic Press, San Diego, 1994).

[12] S. Goh, M. Y. Choi, K. Lee, and K.–m. Kim, Phys. Rev. E **93**, 052309 (2016).

[13] H. A. Makse, S. Havlin, and H. E. Stanley, Nature **377**, 608 (1995); H. A. Makse, J. S. Andrade, Jr., M. Batty, S. Havlin, and H. E. Stanley, Phys. Rev. E **58**, 7054 (1998).

[14] L. Benguigui, Phys. A **219**, 13 (1995).

[15] D. H. Zanette and S. C. Manrubia, Phys. Rev. Lett. **79**, 523 (1997).

[16] C. Andersson, K. Lindgren, S. Rasmussen, and R. White, Phys. Rev. E **66** 026204 (2002).

[17] M. Munz and W. Weidlich, Annals Reg. Sci. 24, 177 (1990); W. Weidlich, *Sociodynamics* (Dover, Mineola, New York, 2000).

[18] J. V. Henderson, *Urban Development: Theory, Fact, and Illusion* (Oxford University Press, Oxford, 1988).

[19] M. Fujita, P. Krugman, and A. J. Venables, *The Spatial Economy* (MIT Press, Cambridge, 1999); M. Fujita, P. Krugman, and T. Mori, Euro. Econ. Rev. **43**, 209 (1999).

[20] R. Louf and M. Barthelemy, Phys. Rev. Lett. **111**, 198702 (2013).

[21] A. Lösch, *Die räumliche Ordnung der Wirtschaft* (Gustav Fischer, Jena, 1940). English translation: *The Economics of Location* (Yale University Press, New Haven, 1954).

[22] T. Tabuchi and J.-F. Thisse, *J. Urban Econ.* **69**, 240 (2011).

[23] K. Ikeda, K. Murota, snd T. Akamatsu, *Int. J. Bifurcation Chaos* **22**, 1230026-1 (2012); K. Ikeda, K. Murota, T. Akamatsu, T. Kono, and Y. Takayama, *J. Econ. Behavior Organization* **99**, 32 (2014).

[24] K. Ikeda and K. Murota, *Bifurcation Theory for Hexagonal Agglomeration in Economic Geography* (Springer-Verlag, Tokyo, 2014).

[25] K. Kirchgässner, *Math. Meth. Appl. Sci.* **1**, 453 (1979).

[26] E. Buzano and M. Golubitsky, *Phil. Trans. R. Soc. A* **308**, 617 (1983).

[27] M. Golubitsky, I. Stewart, and D. G. Schaeffer, *Singularities and Groups in Bifurcation Theory*, Vol. 2 (Springer-Verlag, New York, 1988). M. Golubitsky and I. Stewart, *The Symmetry Perspective* (Birkhäuser, Basel, 2002).

[28] NASA Earth Observatory: http://earthobservatory.nasa.gov/NaturalHazards/view.php?id=79800

[29] The symmetry of an $n \times n$ finite hexagonal lattice is labeled by the group that has the structure of the semidirect product of D_6 by $\mathbb{Z}_n \times \mathbb{Z}_n$, where D_6 is the dihedral group for a hexagonal symmetry and $\mathbb{Z}_n$ is the cyclic group of order n for a translational symmetry. The bifurcation of this group has been studied in [23, 24].

[30] See Supplemental Material for details of methods and spectrum analysis.

[31] E. L. Koschmieder, *Benard Cells and Taylor Vortices* (Cambridge University Press, Cambridge, 1993).

[32] I. Stewart and M. Golubitsky, *Fearful Symmetry: Is God a Geometer?* (Blackwell, Oxford, 1992).

APPENDIX

HEXAGONAL LATTICE AND HEXAGONS OF CHRISTALLER AND LÖSCH

An infinite hexagonal lattice and a finite one are introduced in this section as spatial platforms of hexagonal distributions [24]. The infinite hexagonal lattice is a two-dimensional discretized uniform space that expresses an isotropic infinite plain in central place theory. The finite hexagonal lattice with periodic boundary conditions is advanced as a spatial platform for the investigation of agglomeration patterns in the real world. Hexagonal distributions on these lattices, corresponding to those envisaged by Christaller and Lösch [8, 21], are here explained, parameterized, and classified.

An infinite hexagonal lattice (Fig. A1(a)) comprises a series of regular triangles and covers an infinite two-dimensional domain. This lattice is given as a set of integer combinations of oblique basis vectors $\boldsymbol{\ell}_1 = d(1,0)^\top$ and $\boldsymbol{\ell}_2 = d(-1/2, \sqrt{3}/2)^\top$, where $d > 0$ means the length of these vectors.

A hexagonal distribution of Lösch on the lattice is represented by a sublattice spanned by

$$\boldsymbol{t}_1 = \alpha\boldsymbol{\ell}_1 + \beta\boldsymbol{\ell}_2, \quad \boldsymbol{t}_2 = -\beta\boldsymbol{\ell}_1 + (\alpha-\beta)\boldsymbol{\ell}_2, \tag{A1}$$

where α and β are integer-valued parameters with $(\alpha,\beta) \neq (0,0)$. Figure A1(b) denotes a hexagon on a sublattice for $(\alpha,\beta) = (2,1)$.

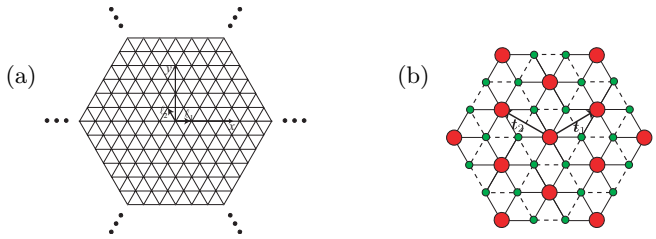

FIG. A1. (a) Hexagonal lattice. (b) A hexagonal distribution for $(\alpha,\beta) = (2,1)$.

The *normalized spatial period* L/d of the sublattice is defined using the (common) length of the basis vectors $\boldsymbol{t}_1$ and $\boldsymbol{t}_2$, and is given by

$$\frac{L}{d} = \sqrt{D} \tag{A2}$$

with $D = \alpha^2 - \alpha\beta + \beta^2$ characterizes the size of the hexagon.

We further introduce a finite hexagonal lattice comprising a system of uniformly distributed $n \times n$ places; see, for example, Fig. A2(a) for the 3×3 hexagonal lattice. Discretized degrees-of-freedom are allocated to each node of the lattice. The periodic boundary conditions are used to express infiniteness and uniformity and to avoid heterogeneity due to the boundaries by spatially repeating the finite lattice periodically to cover an infinite two-dimensional domain (Fig. A2(b)).

The finite lattice, by virtue of its finiteness, can encompass hexagons of finite sizes. A lattice with size $n = 18$, which is employed in this letter, can encompass hexagons with

$$D = 1,\ 3,\ 4,\ 9,\ 12,\ 27,\ 36,\ 81,\ 108,\ 324. \tag{A3}$$

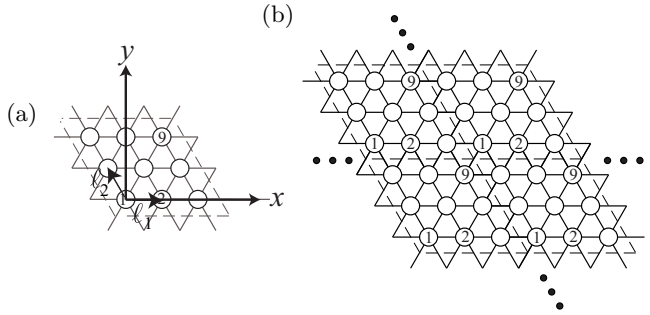

FIG. A2. A system of places on a hexagonal lattice with a periodic boundary condition. (a) 3×3 hexagonal lattice. (b) Spatially repeated 3×3 hexagonal lattices.

GROUP-THEORETIC DOUBLE FOURIER SERIES AND ASSOCIATED SPATIAL PATTERNS

A group-theoretic double Fourier series in oblique coordinates along the finite hexagonal lattice is introduced as a tool to detect spatial patterns [24]. Agglomeration patterns on this lattice that are given by the superposition of the Fourier terms contain hexagonal distributions in central place theory, but also encompass megalopolis patterns, which are beyond the scope of this theory.

We present a group-theoretic double Fourier series for the 18×18 hexagonal lattice that is used in the present spectrum analysis. The basis vectors of this lattice can be decomposed into several subsets which represent patterns with hexagonal symmetry of various kinds.

The population distribution $\boldsymbol{\lambda}$ can be expanded to a group-theoretic double Fourier series as

$$\boldsymbol{\lambda} = \sum_{m \in \mathrm{L}_{\mathrm{hexa}}} \sum_{i=1}^{M(m)} c_i^{(m)} \boldsymbol{q}_i^{(m)} \tag{A4}$$

with Fourier coefficients $c_i^{(m)}$; each m labels a hexagon of a different kind and $M(m)$ is the number of the basis vectors for the label m. There are the patterns with hexagonal symmetry of 37 kinds associated with a set $\mathrm{L}_{\mathrm{hexa}}$ of the labels m of patterns defined by

$$\begin{aligned}\mathrm{L}_{\mathrm{hexa}} = \{&1, 3, 4, 9, 12,\ 27(\mathrm{I}), 27(\mathrm{II}), 27(\mathrm{III}),\ 36(\mathrm{I}), 36(\mathrm{II}),\\ &81(\mathrm{I}), \ldots, 81(\mathrm{VI}),\ 108(\mathrm{I}), \ldots, 108(\mathrm{VI}),\\ &324(\mathrm{I}), \ldots, 324(\mathrm{XV})\}\end{aligned} \tag{A5}$$

TABLE A1. The size D of a hexagon and the number $M(m)$ of basis vectors labeled by $m \in \mathrm{L_{hexa}}$ for $n = 18$.

m	D	$M(m)$
1	1	1
3	3	2
4	4	3
9	9	6
12	12	6
27(I), 27(II), 27(III)	27	6
36(I)	36	6
36(II)	36	12
81(I), 81(II), 81(III)	81	6
81(IV), 81(V), 81(VI)	81	12
108(I), 108(II), 108(III)	108	6
108(IV), 108(V), 108(VI)	108	12
324(I), 324(II), 324(III)	324	6
324(IV), 324(V), ..., 324(XV)	324	12

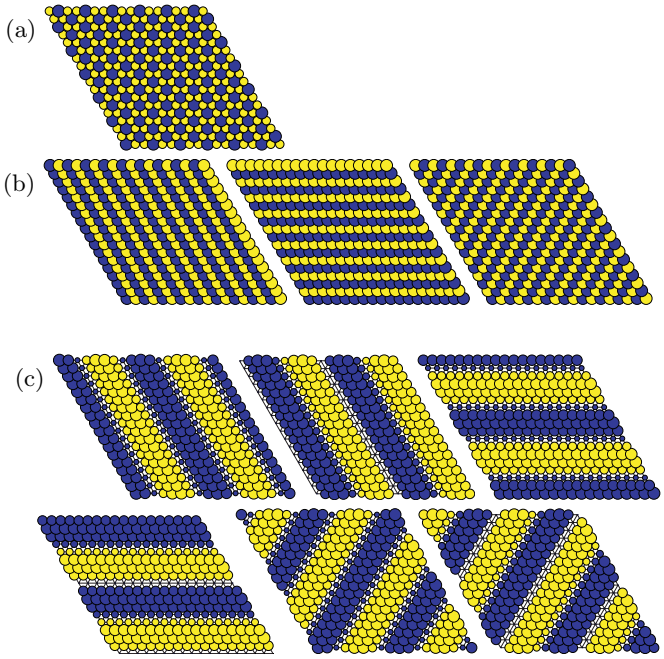

FIG. A3. Spatial patterns expressed by basis vectors. (a) $\boldsymbol{q}_1^{(3)}$. (b) $\boldsymbol{q}_i^{(4)}$ $(i = 1, 2, 3)$. (c) $\boldsymbol{q}_i^{(81(\mathrm{I}))}$ $(i = 1, \ldots, 6)$. A blue circle denotes a positive component, a yellow circle indicates a negative one, and the area of a circle expresses the magnitude of the component.

determining the size D of hexagons (Table A1).

The concrete forms of the basis vectors in (A4) are given by discrete cosine and sine series that are presented later. For example, the basis vector $\boldsymbol{q}_1^{(3)}$ represents a hexagon with $D = 3$ (Fig. A3(a)); the basis vectors $\boldsymbol{q}_i^{(4)}$ $(i = 1, 2, 3)$ and $\boldsymbol{q}_i^{(81(\mathrm{I}))}$ $(i = 1, \ldots, 6)$ express stripe patterns (Figs. A3(b)–(c)).

We assemble the terms corresponding to a particular m in (A4) as

$$\boldsymbol{q}^{(m)} = \sum_{i=1}^{M(m)} c_i^{(m)} \boldsymbol{q}_i^{(m)}. \tag{A6}$$

This vector $\boldsymbol{q}^{(m)}$ is not necessarily an equilibrium that bifurcates from a uniform state for randomly chosen coefficients $c_i^{(m)}$, but can be associated with a hexagon for appropriately chosen $c_i^{(m)}$, its size being implied by m.

Then the double Fourier series in (A4) is rewritten as

$$\boldsymbol{\lambda} = \sum_{m \in \mathrm{L_{hexa}}} \boldsymbol{q}^{(m)}. \tag{A7}$$

A group-theoretic spectrum analysis procedure proposed herein proceeds as follows: (i) Observe the squared magnitudes $||\boldsymbol{q}^{(m)}||^2$ $(m \in \mathrm{L_{hexa}})$ of these vectors with the Euclidean norm $||\cdot||$. (ii) Detect the wave numbers m of the predominant spectra (except for that of the uniform population $\boldsymbol{q}^{(1)}$). (iii) Inspect the associated spatial patterns $\boldsymbol{q}^{(m)}$.

Of the possible bifurcating patterns from a uniform state on the 18×18 hexagonal lattice, we focus on those with hexagonal symmetry that are given as [24]:

$$\boldsymbol{q}_{\mathrm{hexa}}^{(m)} = \begin{cases} \boldsymbol{q}^{(3)} & \text{for } m = 3 \text{ with } M(m) = 2, \\ \boldsymbol{q}_1^{(4)} + \boldsymbol{q}_2^{(4)} + \boldsymbol{q}_3^{(4)} & \text{for } m = 4 \text{ with } M(m) = 3, \\ \boldsymbol{q}_1^{(m)} + \boldsymbol{q}_3^{(m)} + \boldsymbol{q}_5^{(m)} & \text{for } m\text{'s with } M(m) = 6, \\ \displaystyle\sum_{i=1}^{6} \boldsymbol{q}_{2i-1}^{(m)} & \text{for } m\text{'s with } M(m) = 12. \end{cases} \tag{A8}$$

There are a set of 37 patterns with hexagonal symmetry (Figs. 3 and A4). The patterns with $m = 3$, 4, 9, 12, 27(I), 36(I), 81(I), 108(I), and 324(I) represent spatially-repeated hexagonal patterns (Figs. 3(a) and A4). The patterns with smaller m values have a larger number of first level places.

Basis vectors for 18×18 hexagonal lattice

The rearranged double Fourier series for the 18×18 hexagonal lattice is presented [24]. The coordinate of a place on the $n \times n$ hexagonal lattice is given by

$$\boldsymbol{x} = n_1 \boldsymbol{\ell}_1 + n_2 \boldsymbol{\ell}_2, \qquad (n_1, n_2 = 0, 1, \ldots, n-1),$$

and the places are indexed by (n_1, n_2). Accordingly, the population distribution vector is indexed as

$$\boldsymbol{\lambda} = (\lambda_{n_1 n_2} \mid n_1, n_2 = 0, \ldots, n-1).$$

For a vector

$$(g(n_1, n_2) \mid n_1, n_2 = 0, 1, \ldots, n-1)$$

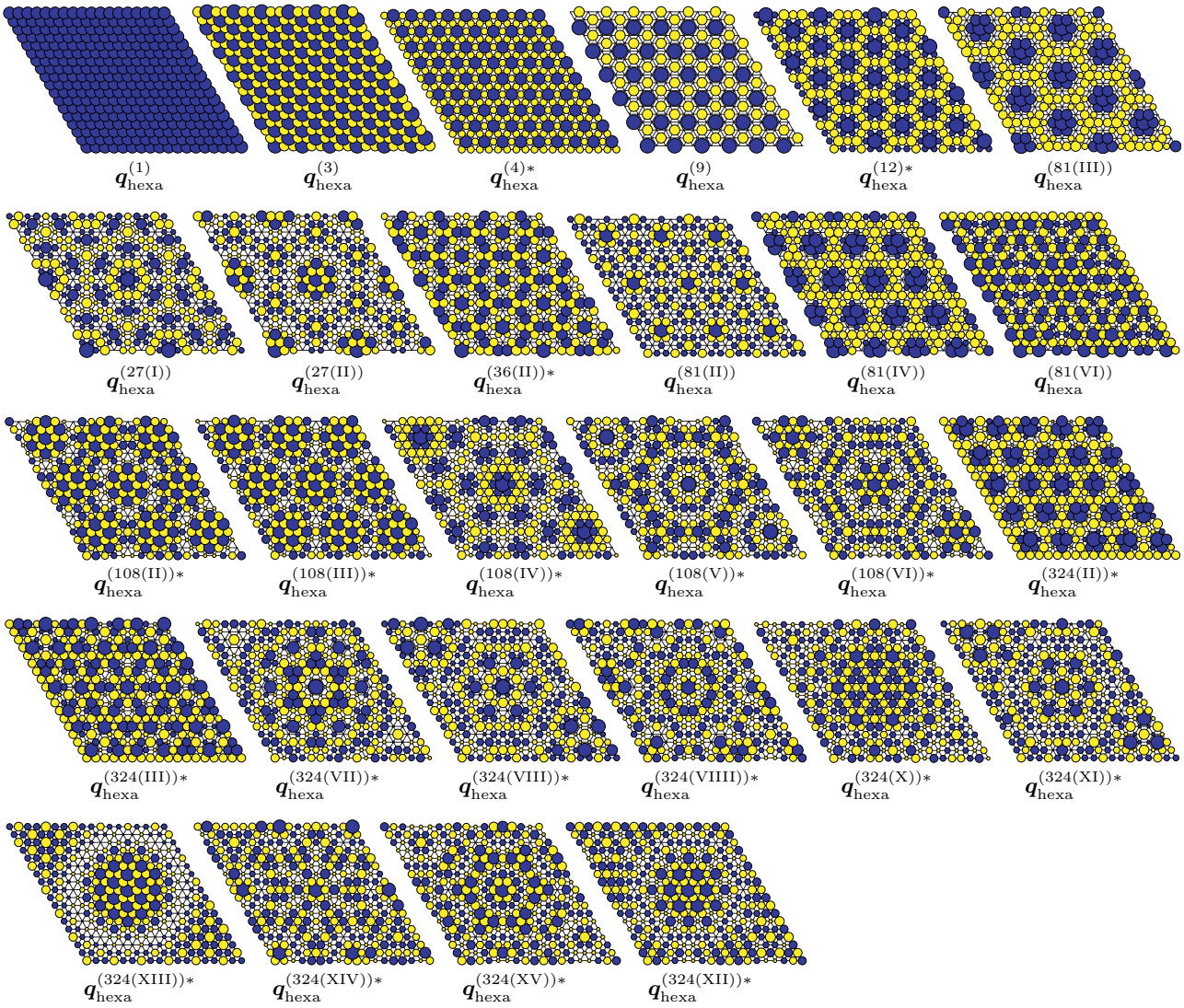

FIG. A4. Patterns with hexagonal symmetry other than those given in Fig. 1. Hexagons centered at $(n_1, n_2) = (9, 9)$ are expressed by $\boldsymbol{q}^{(m)*}_{\rm hexa}$; a blue circle denotes a positive component, a yellow circle indicates a negative one, and the area of a circle expresses the magnitude of the component.

on the lattice with $g(n_1, n_2)$ being the (n_1, n_2)-component, we use the notation $\langle g(n_1, n_2)\rangle$ for its normalization ($n = 18$):

$$\langle g(n_1,n_2)\rangle = (g(n_1,n_2)/\Big(\sum_{i=0}^{n-1}\sum_{j=0}^{n-1} g(i,j)^2\Big)^{1/2} \mid n_1,n_2 = 0,1,\ldots,n-1).$$

First, the basis vectors $\boldsymbol{q}^{(m)}_1, \ldots, \boldsymbol{q}^{(m)}_{M(m)}$ for $m = 1$, 3 and 4 are given by

$$\boldsymbol{q}^{(1)}_1 = \frac{1}{6}(1,\ldots,1)^\top,$$
$$\left[\boldsymbol{q}^{(3)}_1, \boldsymbol{q}^{(3)}_2\right] = \left[\langle\cos(2\pi(n_1-2n_2)/3)\rangle, \langle\sin(2\pi(n_1-2n_2)/3)\rangle\right],$$
$$\left[\boldsymbol{q}^{(4)}_1, \boldsymbol{q}^{(4)}_2, \boldsymbol{q}^{(4)}_3\right] = \left[\langle\cos(\pi n_1)\rangle, \langle\cos(\pi n_2)\rangle, \langle\cos(\pi(n_1-n_2))\rangle\right].$$

The basis vectors for $m = 9$, 36(I), 81(I), 81(II), 81(III), 324(I), 324(II), and 324(III) are given by

$$\left[\boldsymbol{q}^{(m)}_1, \ldots, \boldsymbol{q}^{(m)}_6\right] = [\ \langle\cos(2\pi k\ n_1/n)\rangle,\ \langle\sin(2\pi k\ n_1/n)\rangle, \langle\cos(2\pi k(-n_2)/n)\rangle,\ \langle\sin(2\pi k(-n_2)/n)\rangle, \langle\cos(2\pi k(-n_1+n_2)/n)\rangle,\ \langle\sin(2\pi k(-n_1+n_2)/n)\rangle\ ]$$

with $n = 18$ and the correspondence

m	9	36(I)	81(I)	81(II)	81(III)	324(I)	324(II)	324(III)
k	6	3	2	4	8	1	5	7

The basis vectors for $m = 12$, 27(I), 27(II), 27(III),

108(I), 108(II), and 108(III) are given by

$$\begin{aligned}&\left[\boldsymbol{q}_1^{(m)},\ldots,\boldsymbol{q}_6^{(m)}\right]\\&=[\ \langle\cos(2\pi k(n_1+n_2)/n)\rangle,\ \langle\sin(2\pi k(n_1+n_2)/n)\rangle,\\&\quad\langle\cos(2\pi k(n_1-2n_2)/n)\rangle,\ \langle\sin(2\pi k(n_1-2n_2)/n)\rangle,\\&\quad\langle\cos(2\pi k(-2n_1+n_2)/n)\rangle,\ \langle\sin(2\pi k(-2n_1+n_2)/n)\rangle\ ]\end{aligned}$$

with the correspondence

m	12	27(I)	27(II)	27(III)	108(I)	108(II)	108(III)
k	3	2	4	8	1	5	7

The basis vectors for $m = 12$, 36(II), 81(IV), 81(V), 81(VI), 108(IV), 108(V), 108(VI), 324(IV), ..., 324(XV) are given by

$$\begin{aligned}&\left[\boldsymbol{q}_1^{(m)},\ldots,\boldsymbol{q}_{12}^{(m)}\right]\\&=[\ \langle\cos(2\pi(kn_1+\ell n_2)/n)\rangle,\\&\quad\langle\sin(2\pi(kn_1+\ell n_2)/n)\rangle,\\&\quad\langle\cos(2\pi(\ell n_1-(k+\ell)n_2)/n)\rangle,\\&\quad\langle\sin(2\pi(\ell n_1-(k+\ell)n_2)/n)\rangle,\\&\quad\langle\cos(2\pi(-(k+\ell)n_1+kn_2)/n)\rangle,\\&\quad\langle\sin(2\pi(-(k+\ell)n_1+kn_2)/n)\rangle,\\&\quad\langle\cos(2\pi(kn_1-(k+\ell)n_2)/n)\rangle,\\&\quad\langle\sin(2\pi(kn_1-(k+\ell)n_2)/n)\rangle,\\&\quad\langle\cos(2\pi(\ell n_1+kn_2)/n)\rangle,\\&\quad\langle\sin(2\pi(\ell n_1+kn_2)/n)\rangle,\\&\quad\langle\cos(2\pi(-(k+\ell)n_1+\ell n_2)/n)\rangle,\\&\quad\langle\sin(2\pi(-(k+\ell)n_1+\ell n_2)/n)\rangle\ ]\end{aligned}$$

with the correspondence

m	36(II)	81(IV)	81(V)	81(VI)
(k,ℓ)	$(6,3)$	$(4,2)$	$(6,2)$	$(6,4)$

108(IV)	108(V)	108(VI)
$(4,1)$	$(5,2)$	$(7,1)$

m	324(IV)–324(X)
(k,ℓ)	$(2,1),(3,1),(3,2),(4,3),(5,1),(5,3),(5,4)$

m	324(XI)–324(XV)
$(6,1),(6,5),(7,2),(7,3),(8,1)$	

SPECTRUM ANALYSIS OF SOUTHERN GERMANY

In the spectrum analysis of Southern Germany, the population data (Table A2) were taken from the City Population website (http://www.citypopulation.de/), which is based on original sources (Table A3).

TABLE A2. City population size classification (2011/5/9) (city population is based on administrative division).

Name of center	Name of City	Population
A-center ($\lambda \geq 1,000,000$)	München Stadt	1,348,335
B-center	Frankfurt am Main	667,925
($400,000 \leq \lambda < 1,000,000$)	Stuttgart	585,890
	Nürnberg	486,314
	Strasbourg	482,384
C-center ($\lambda < 400,000$)	Bezirk Zurich	372,857
	Kempton (Allgäu)	64,078

TABLE A3. Original sources of population data.

Country	Data bank and Internet address
Germany	Statistisches Bundesamt Deutschland
	https://www.destatis.de/EN/Homepage.html
Austria	Statistik Austria
	http://www.statistik.at/web_de
	/statistiken/index.html
France	Institut National de la Statistique et
	des Études Économiques
	http://www.insee.fr/fr/
Switzerland	Swiss Statistics
	http://www.bfs.admin.ch/bfs
	/portal/en/index.html
Luxembourg	Le Portail des Statistiques du Luxembourg
	http://www.statistiques.public.lu/en/index.html

SPECTRUM ANALYSIS OF EASTERN USA

The 2014 population data of Eastern USA were acquired from original sources listed in Table A4. Based on population size, cities were classified from an A-center at New York City, B-centers at Chicago, Dallas, Houston, Washington, and Atlanta, to F-centers (Tables A5 and A6). The Eastern USA was divided into Gulf Coast,

South Atlantic, East and West North Central, and Middle Atlantic Regions (Fig. A5). By the spectrum analysis of the population data, we found the 18 rhombic domains accommodating hexagonal and megalopolis patterns of cities (Fig. A5).

TABLE A4. Original sources of population data.

Country	Data bank and Internet address
USA	US Census Bureau http://www.census.gov/
Canada	Statistics Canada http://www.statcan.gc.ca/start-debut-eng.html

TABLE A5. City population size classification A to E (2014/7/1). (Metropolitan and micropolitan statistical areas are geographic entities delineated by the Office of Management and Budget (OMB) for use by federal statistical agencies in collecting, tabulating, and publishing federal statistics.)

Name of center	Name of city	Population
A-center ($\lambda \geq 10,000,000$)	New York City - Newark - Jersey City	20,092,883
B-center ($5,000,000 \leq \lambda < 10,000,000$)	Chicago - Naperville - Elgin	9,554,598
	Dallas - Fort Worth - Arlington	6,954,330
	Houston - The Woodlands - Sugar Land	6,490,180
	Washington - Arlington - Alexandria	6,033,737
	Atlanta - Sandy Springs - Roswell	5,614,323
C-center ($3,500,000 \leq \lambda < 5,000,000$)	Boston - Cambridge - Newton	4,732,161
	Detroit - Warren - Dearborn	4,296,611
D-center ($2,000,000 \leq \lambda < 3,500,000$)	St. Louis	2,806,207
	Charlotte - Concord - Gastonia	2,380,314
	Pittsburgh	2,355,968
	San Antonio - New Braunfels	2,328,652
	Cincinnati	2,149,449
	Kansas City	2,071,133
	Cleveland - Elyria	2,063,598
E-center ($1,000,000 \leq \lambda < 2,000,000$)	Columbus (OH)	1,994,536
	Indianapolis - Carmel - Anderson	1,971,274
	Nashville - Davidson - Murfreesboro - Franklin	1,792,649
	Virginia Beach - Norfolk - Newport News	1,716,624
	Milwaukee - Waukesha - West Allis	1,572,245
	Jacksonville	1,419,127
	Memphis	1,343,230
	Oklahoma City	1,336,767
	Louisville/Jefferson County	1,269,702
	Richmond	1,260,029
	New Orleans - Metairie	1,251,849
	Raleigh	1,242,974
	Birmingham - Hoover	1,143,772
	Grand Rapids - Wyoming	1,027,703

TABLE A6. City population size classification F (2014/7/1). (Metropolitan and micropolitan statistical areas are geographic entities delineated by the Office of Management and Budget (OMB) for use by federal statistical agencies in collecting, tabulating, and publishing federal statistics.)

Name of center	Name of city	Population
F-center	Tulsa	969,224
$(100,000 \leq \lambda < 1,000,000)$	Omaha - Council Bluffs	904,421
	Greenville - Anderson - Mauldin	862,463
	Knoxville	857,585
	Columbia (SC)	800,495
	Greensboro - High Point	746,593
	Little Rock - North Little Rock - Conway	729,135
	Charleston - North Charleston	727,689
	Wichita	641,076
	Des Moines - West Des Moines	611,549
	Toledo	607,456
	Augusta - Richmond County	583,632
	Jackson	577,564
	Chattanooga	544,559
	Lexington - Fayette	494,189
	Pensacola - Ferry Pass - Brent	474,081
	Springfield	452,297
	Shreveport - Bossier City	445,142
	Huntsville	441,086
	Myrtle Beach - Conway - North Myrtle Beach	417,668
	Tallahassee	375,751
	Montgomery	373,141
	Savannah	372,708
	Huntington - Ashland	363,325
	Evansville	315,162
	Columbus (GA-AL)	314,005
	Macon	230,450
	Charleston	222,878
	Johnson City	201,091
	Columbia (MO)	172,717
	Terre Haute	171,480
	Albany	154,925
	Dothan	148,095
	Valdosta	143,317
	Anniston - Oxford - Jacksonville	115,916

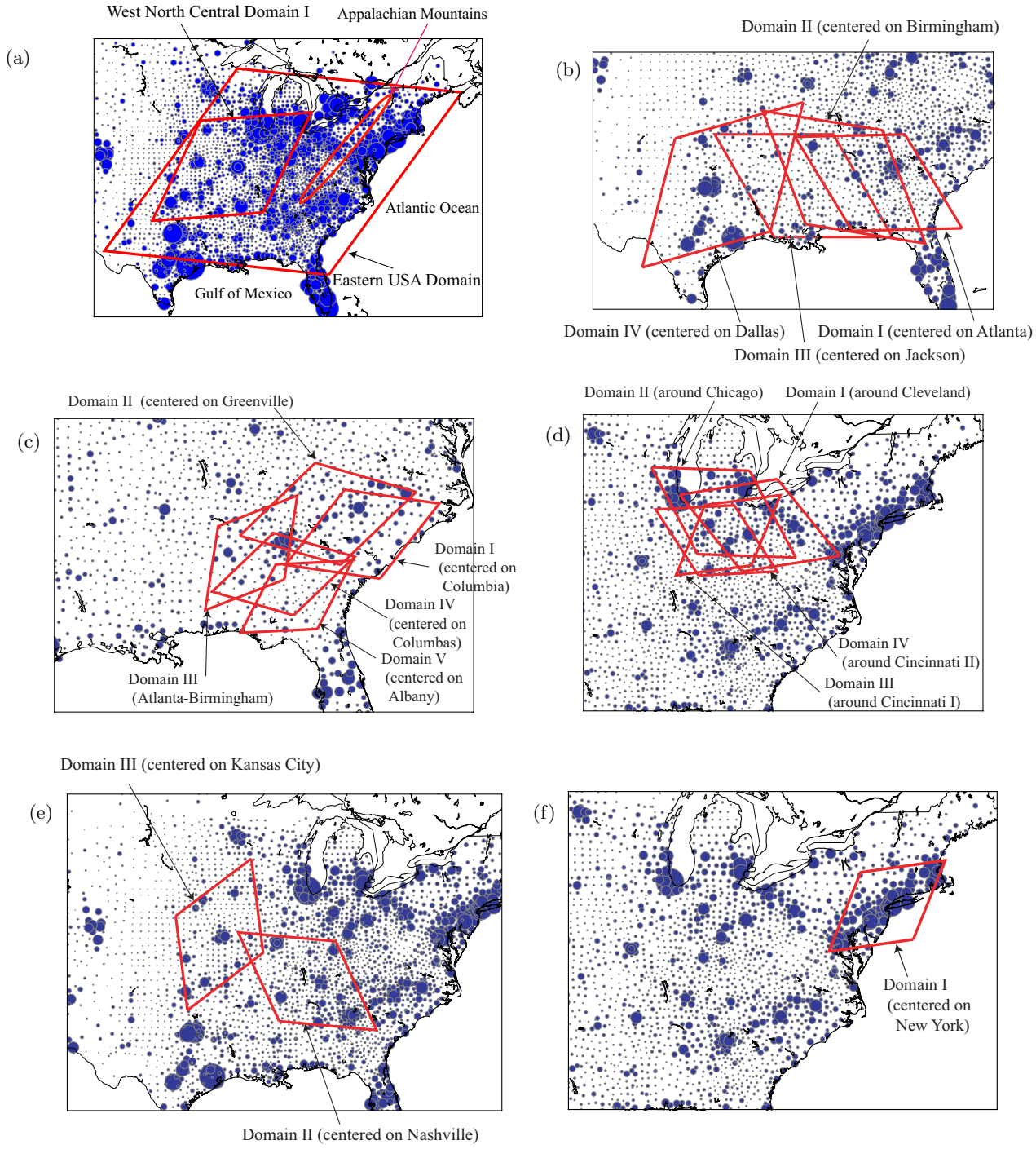

FIG. A5. Rhombic domains for the spectrum analysis drawn on population maps in Eastern USA. (a) Eastern USA Domain and West North Central Domain I. (b) Gulf Coast Region (Domains I–IV). (c) South Atlantic Region (Domains I–V). (d) East North Central Region (Domains I–IV). (e) West North Central Region (Domains II–III). (f) Middle Atlantic Region (Domain I).

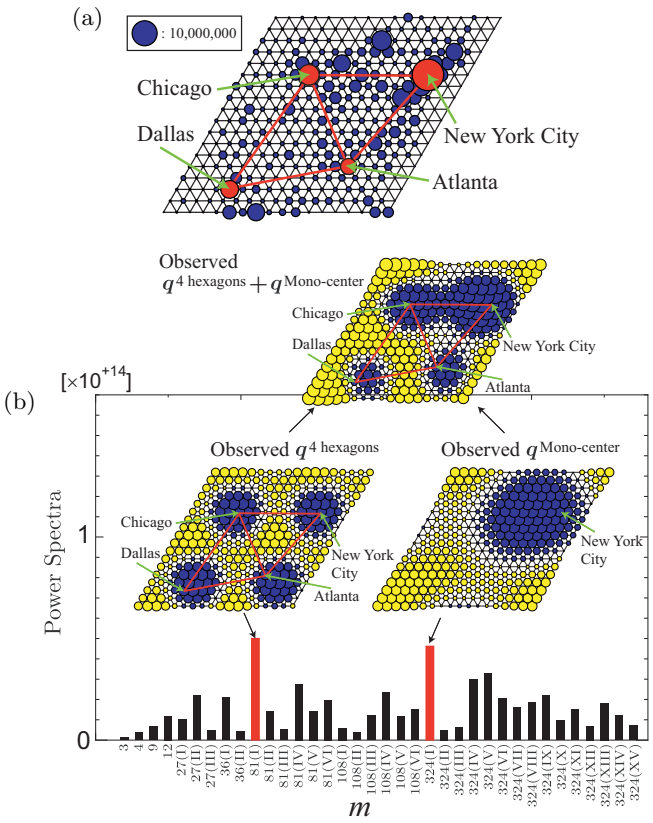

FIG. A6. Spectrum analysis for Eastern USA Domain. (a) Population distributions and a distribution of cities. The area of a circle denotes the population size and a series of red lines denotes the distribution of cities. (b) Power spectra of the squared magnitudes $||\boldsymbol{q}^{(m)}||^2$ of the assembled Fourier terms and spatial patterns of the predominant spectra $\boldsymbol{q}^{4\ \text{hexagons}}$ and $\boldsymbol{q}^{\text{Mono-center}}$ for this region. A blue circle denotes a positive component, a yellow circle indicates a negative one, and the area of a circle expresses the magnitude of the component.

For Eastern USA Domain (Figs. A5(a) and Fig. A6(a)), we found two competing strong spectra for $\boldsymbol{q}^{4\ \text{hexagons}} \equiv \boldsymbol{q}^{(81(\text{I}))}$ and $\boldsymbol{q}^{\text{Mono-center}} \equiv \boldsymbol{q}^{(324(\text{I}))}$ (Fig. A6(b)). The pattern $\boldsymbol{q}^{4\ \text{hexagons}}$ displays a 2×2 hexagonal pattern comprising a rhombic-shape with four cities: New York City, Chicago, Dallas, and Atlanta, whereas $\boldsymbol{q}^{\text{Mono-center}}$ displays a mono-center at New York City. These two patterns are superposed to arrive at $\boldsymbol{q}^{4\ \text{hexagons}} + \boldsymbol{q}^{\text{Mono-center}}$ at the top of Fig. A6(b), which can be interpreted as a two-level hierarchy (Fig. 7(b)), comprising an A-center at New York City and three B-centers.

The results of the spectrum analysis of other regions are presented in Figs. A7–A10. The largest spectrum (except for that of the uniform state for $m = 1$) is associated with the megalopolis pattern $\boldsymbol{q}^{\text{Magalopolis}}$, except for Middle Atlantic Domain I, for which $\boldsymbol{q}^{3\ \text{hexagons}}$ is predominant. The results for the four domains in Gulf Coast Region (Fig. A7) are used to arrive at the clearest hexagonal distribution of cities (Figs. 6(c)–(d)). Those for the five domains in South Atlantic Region (Fig. A8) are assembled to arrive at the fine hexagonal distribution (Fig. 7(a)). Those in East North Central Region (Fig. A9) are used to arrive at the T-shaped distribution in Fig. 7(a). West North Central Domains II around Nashville is a hub of city network connecting three regions of the Gulf Coast, the South Atlantic, and the East North Central (the top left of Figs. A10(a)–(b)). Middle Atlantic Domain I has a long narrow network from Boston to Washington via New York City (Fig. 7(c) and the bottom of Figs. A10(a)–(b)).

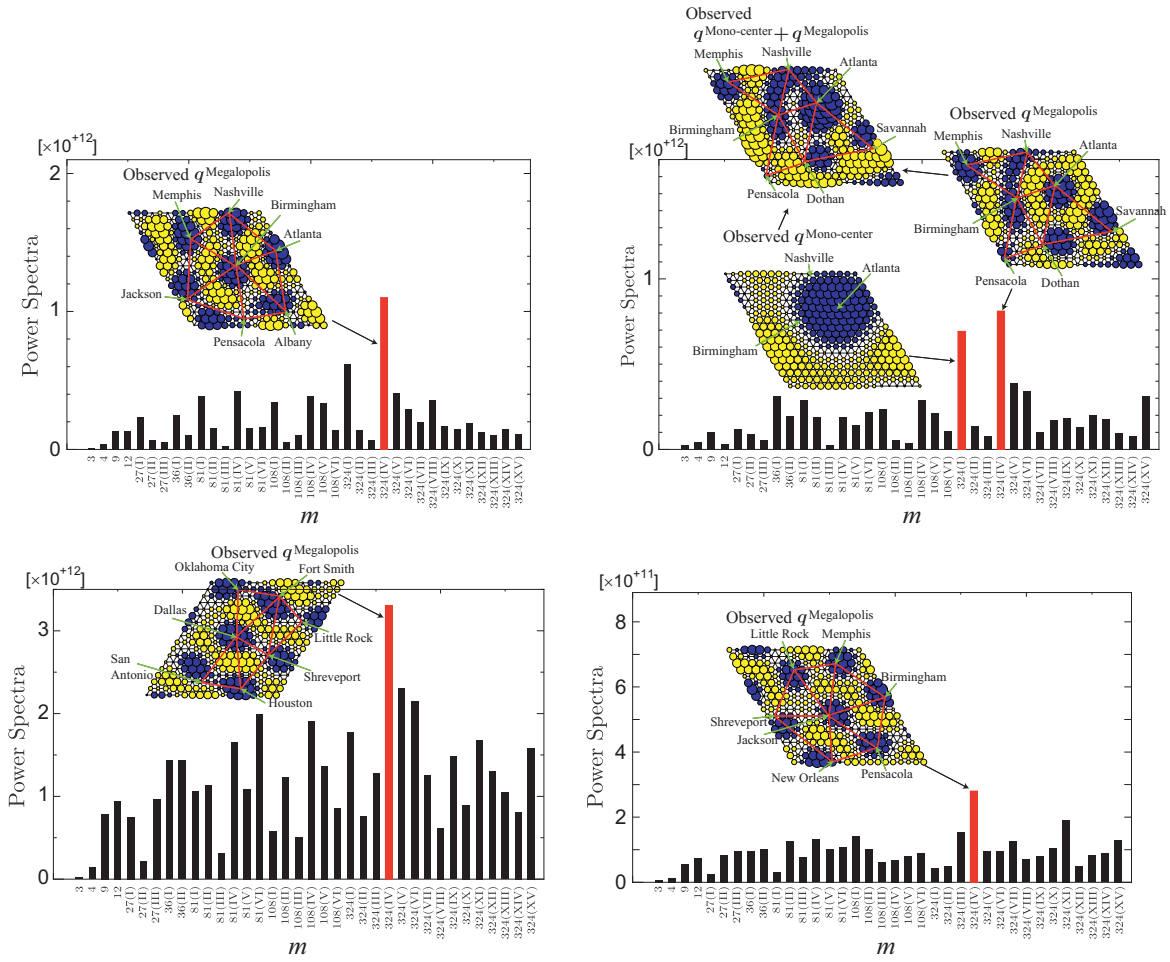

FIG. A7. Power spectra and the spatial patterns of the predominant spectrum $\boldsymbol{q}^{\text{Megalopolis}}$ for the four domains in Gulf Coast Region. A blue circle denotes a positive component, a yellow circle indicates a negative one, and the area of a circle expresses the magnitude of the component.

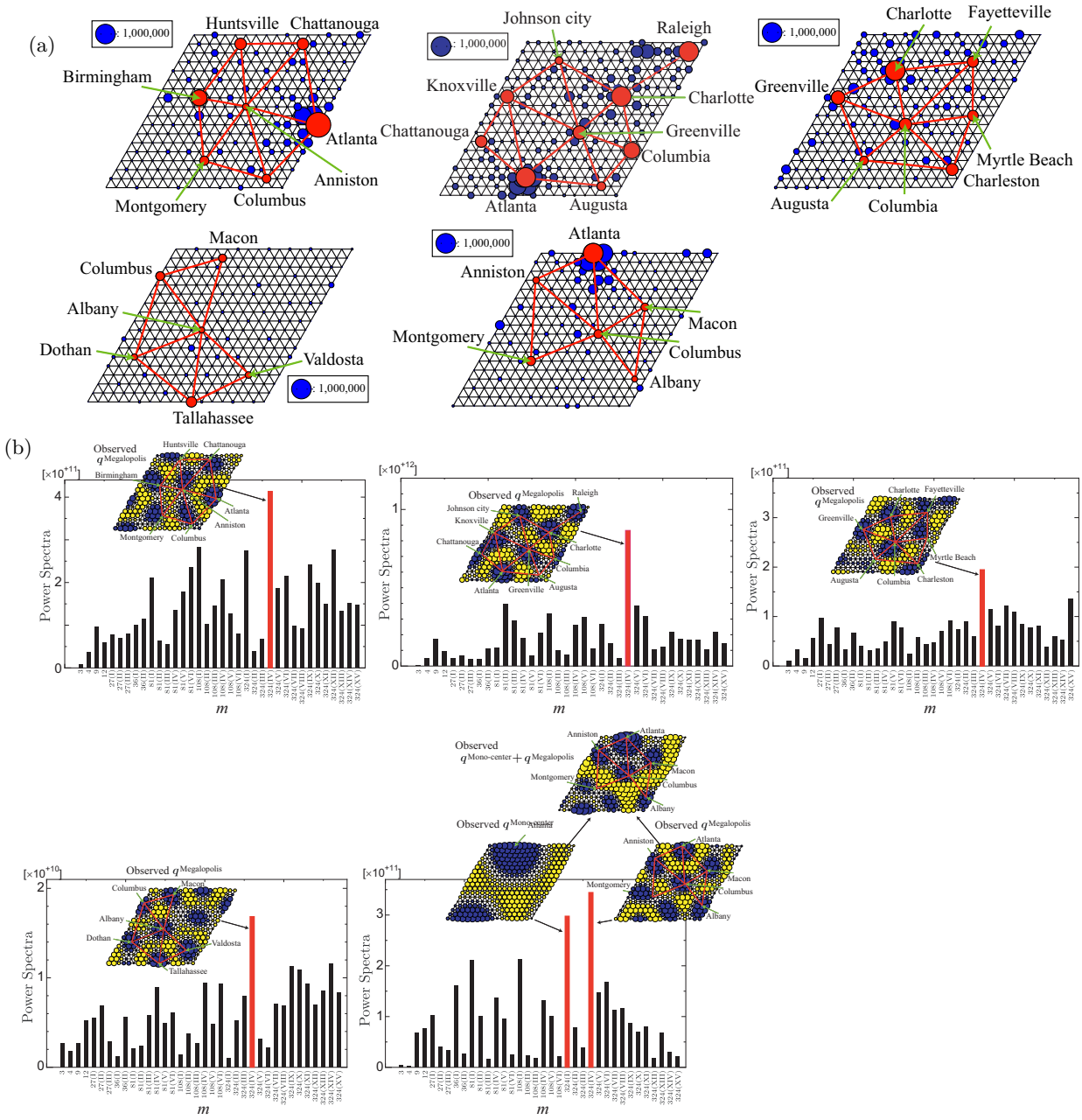

FIG. A8. Spectrum analysis for the five domains in South Atlantic Region. (a) Population distributions and a distribution of cities. The area of a circle denotes the population size and a series of red lines denotes the distribution of cities. (b) Power spectra and the spatial patterns of the predominant spectrum $\boldsymbol{q}^{\text{Megalopolis}}$. A blue circle denotes a positive component, a yellow circle indicates a negative one, and the area of a circle expresses the magnitude of the component.

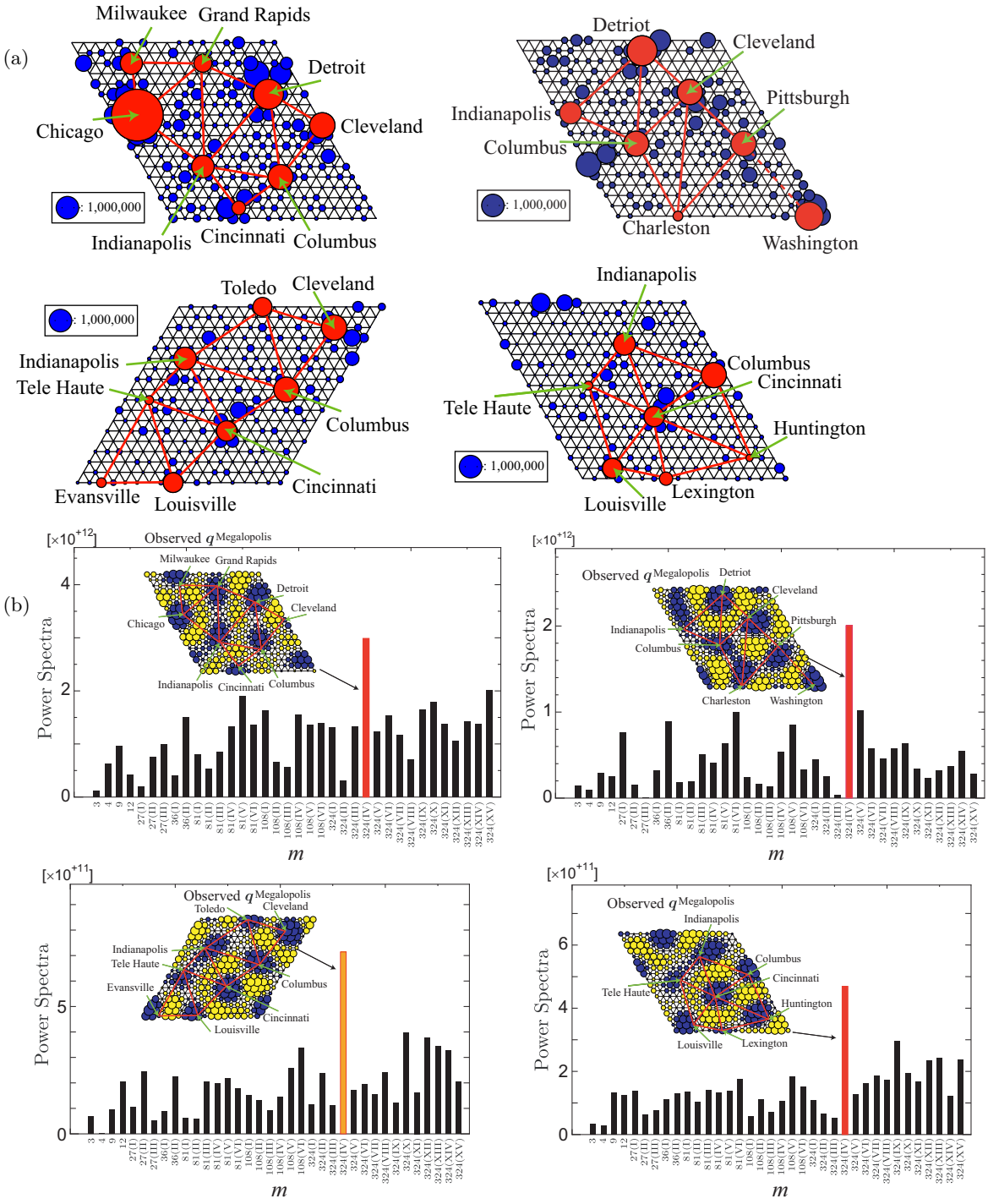

FIG. A9. Spectrum analysis for the four domains in East North Central Region. (a) Population distributions and a distribution of cities. The area of a circle denotes the population size and a series of red lines denotes the distribution of cities. (b) Power spectra and the spatial patterns of the predominant spectrum $\boldsymbol{q}^{\text{Megalopolis}}$. A blue circle denotes a positive component, a yellow circle indicates a negative one, and the area of a circle expresses the magnitude of the component.

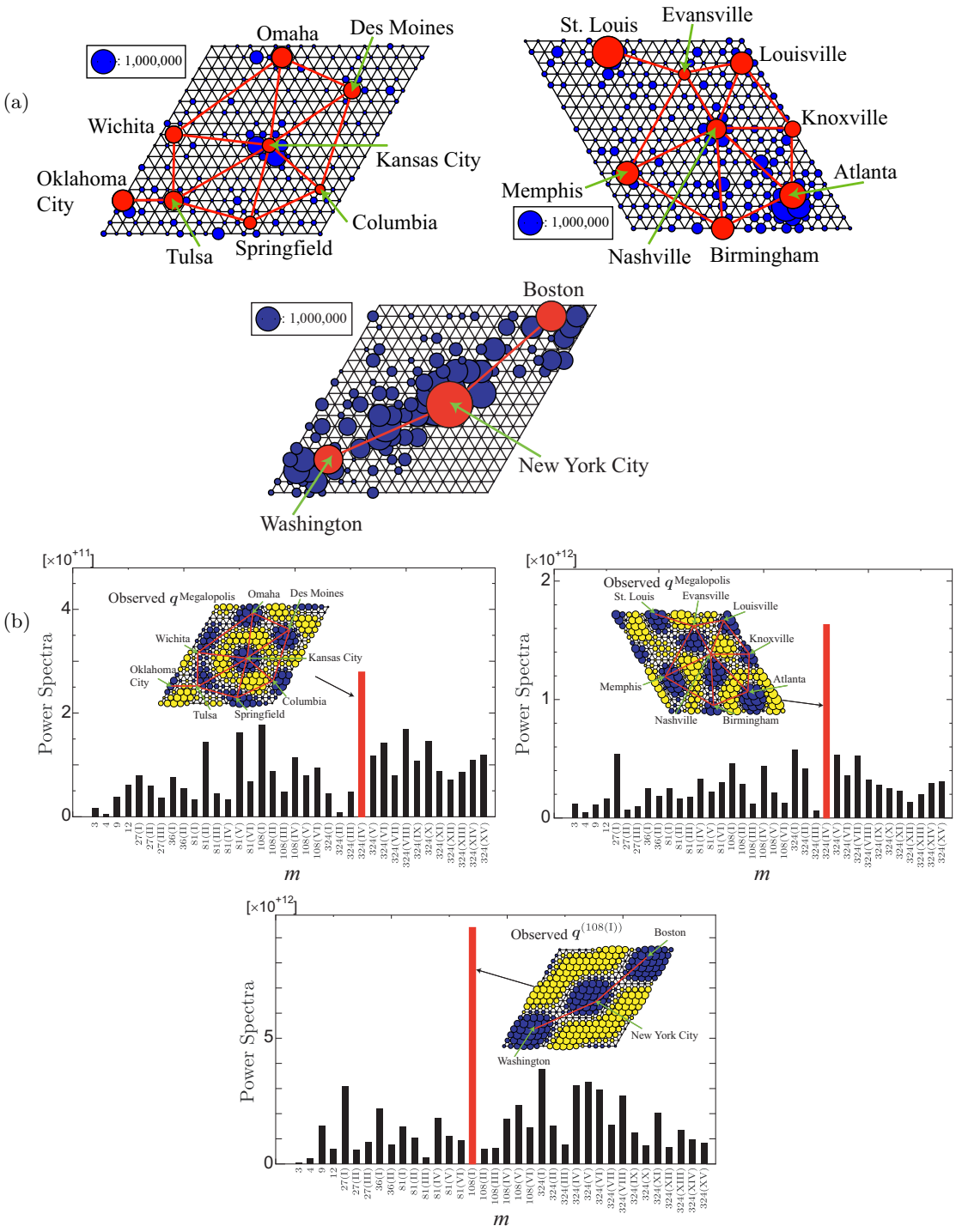

FIG. A10. Spectrum analysis for East North Central Domains II and III and Middle Atlantic Domain I. (a) Population distributions and a distribution of cities. The area of a circle denotes the population size and a series of red lines denotes the distribution of cities. (b) Power spectra and spatial patterns of predominant spectra. A blue circle denotes a positive component, a yellow circle indicates a negative one, and the area of a circle expresses the magnitude of the component.